

An InGaAsP/InP Integration Platform with Low Loss Deeply Etched Waveguides and Record SOA RF-linearity

Erik J. Norberg, Robert S. Guzzon, John S. Parker, Steven P. DenBaars, Larry A. Coldren

Department of Electrical and Computer Engineering and Department of Materials, University of California Santa

Barbara, Santa Barbara, CA 93106

norberg@ece.ucsb.edu

Abstract: We present a novel InGaAsP/InP integration platform that simultaneously achieves high saturation power and low deeply etched waveguide loss, while requiring only a single blanket regrowth. RF-linearity of SOAs was characterized with record performance.

OCIS codes: (250.5300) Photonic integrated circuits; (250.4480) Optical amplifier; (130.3130) Integrated optics materials.

1. Introduction and Background

High saturation power (P_s) optical amplifiers find wide use in optical communication systems, mode-locked lasers and various RF-photonics applications [1-3]. For monolithic integration, low loss waveguides are advantageous in maintaining good signal integrity, and avoiding use of excess gain leading to worse overall noise figure and increased power consumption. In particular, integrated RF-photonics devices, demand both low passive loss and high P_s to achieve a high spur-free dynamic range (SFDR) [1,3].

For semiconductor optical amplifiers (SOAs), P_s is increased by reducing carrier lifetime, τ , or differential gain, a , or by reducing the photon density inside of the quantum wells. The former is reduced by operating the SOA at high current density, which is ultimately limited by device heating. The photon density can be decreased either by increasing the area of the active region (wd) or reducing Γ . Much has been reported on tapering the waveguide width to increase P_s . However, this typically only finds use as in laser amplifiers since integration with other components is difficult when using such wide waveguides. Also, using slab-coupled waveguides and also very large optical mode profiles, watt-class amplifiers have been successfully demonstrated [4]. However, neither the widely tapered waveguides nor the slab-coupled waveguides can be easily integrated with other functional chip components such as modulators, waveguide bends, lateral couplers or lasers. By reducing Γ , Raring *et al.* was able to integrate many functions on chip while achieving P_s in the 20 dBm range, by using a separate re-growth of low confinement quantum wells with a quantum well intermixing (QWI) integration platform [5].

For active InGaAsP/InP integration, free-carrier absorption (FCA) is typically the dominating contribution to propagation loss in passive sections. This can be eliminated by using additional butt-joint or complicated selective area re-growth schemes; however, either option significantly complicates the fabrication process.

In this work we have developed a modified single blanket re-growth offset quantum well (OQW) integration platform, which simultaneously achieves high P_s active regions and low-loss passive sections. Furthermore, by utilizing high confinement deeply etched waveguides, very compact integration and wide a variety of photonic integrated circuits (PICs) such as resonator structures are supported. We demonstrate excellent DC performance (G_o , P_s and passive loss) that matches well to theoretical simulations, and the SOAs are also characterized in terms of RF-linearity with state of the art results.

2. Epitaxial Design and Simulations

In order to increase P_s , we follow the general approach of Raring *et al.*[5], to reduce Γ by placing the quantum wells further out in the tail of the optical mode, increasing saturation power while decreasing the modal gain. Fig.1(a) illustrates our integration platform with a confinement tuning (CT)-layer inserted between the transverse waveguide and the active region. The waveguide consist of a 1.36Q:Si or 1.3Q:Si layer, and the active regions consists of five 65 Å thick 1.65Q material at 0.9% compressive strain surrounded by six 80 Å thick 1.22Q barriers at -0.2% tensile strain. A 170 Å 1.22Q -0.2% separate confinement heterostructure (SCH) layer is used on the p-side. We have investigated different thicknesses of the CT-layer to tune the Γ and achieve different levels of loss reduction.

P_s and the unsaturated gain, $G_o = e^{\Gamma g_o - \langle \alpha_i \rangle}$ (g_o is unsaturated material gain and $\langle \alpha_i \rangle$ is active loss), have been simulated in Fig.1(b), as a function of confinement factor and various numbers of quantum wells. The simulation uses the well-known equation for P_s , see e.g. [5], together with material parameters found from broad area laser measurements. It is clear that more quantum wells give a higher P_s for a constant confinement factor. This is of course due to the increased active region area (d). However, when lowering Γ (increasing CT-layer thickness), the first order transverse mode will eventually start guiding, a situation which cannot be tolerated. Thus, the P_s curves in

Fig. 1(b) are discontinuities where the design is no longer single mode, the point at which this occurs was separately established by calculating the optical mode spectrum for each design, using the finite-difference method (FDM).

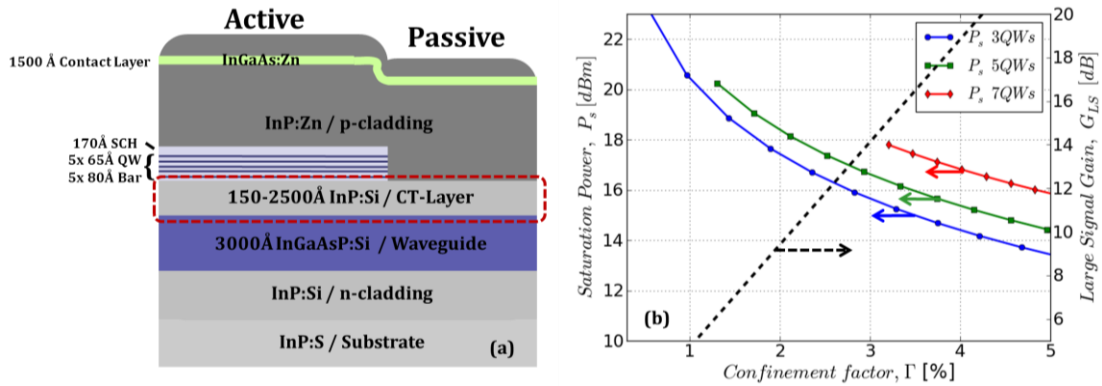


Fig. 1. (a) Schematic drawing of the integration platform, with the CT-layer highlighted. (b) P_s (solid lines) and G_{LS} (dashed line) simulated as a function of Γ and various numbers of quantum wells.

Passive waveguide sections are produced by patterning and selectively etching away the quantum wells in active regions, and a single blanket re-growth of InP:Zn p-cladding and InGaAs:Zn contact layer is then applied. The CT-layer of InP:Si is left in passive regions, in favor of the lower FCA of Si-doping compared with Zn-doping. We have simulated the reduction in passive loss using the CT-layer in Fig. 2(c). This was done by calculating the various modal overlaps with regions of different doping (again by solving the mode with FDM), and using absorption coefficients for Si- and Zn-doping of $9 \cdot (n/1e17) [\text{cm}^{-1}]$ and $20 \cdot (p/1e18) [\text{cm}^{-1}]$ [6], where n and p are the doping concentration in $[\text{cm}^{-3}]$.

3. Fabrication and Characterization of Deeply Etched Waveguides

The InGaAsP/InP epitaxial base structure as well as the p-cladding blanket regrowth was grown with metal organic chemical vapor deposition (MOCVD). Deeply etched waveguides were defined using standard i-line stepper lithography and a bi-layer $\text{SiO}_2\text{:Cr}$ hard mask, followed by an $\text{H}_2\text{Cl}_2\text{:Ar}$ based inductively coupled plasma (ICP) etch [Parker]. Fig. 2(a) and (b) show a cross section of an active and passive deeply etched waveguide section, from the 250 nm CT-layer design; very anisotropic and fairly smooth sidewalls are evident. All the waveguides are kept $3.0 \mu\text{m}$ wide, and as we have previously shown when integrated with multi-mode interference (MMI) couplers single mode operation is still achieved [3].

The passive waveguide loss was found by fiber coupling amplified spontaneous emission (ASE) into 3 mm long waveguide cavities with cleaved mirror facets, then measuring the throughput extinction ratio with an optical spectrum analyzer (OSA), and using the standard Fabry-Pérot method with facet power reflection of 0.32 assumed. Deeply etched passive waveguides for three different CT-layer designs is compared in Fig 2(c). The loss is reduced by about a factor of two going from a standard OQW (15 nm CT-layer) to the 250 nm CT-layer design. The loss of the latter design is $\sim 3.5 \text{ dB/cm}$, which is low loss for deeply etched waveguides. The total simulated loss was fitted to measurement by adding a constant scattering (and/or interband absorption) loss contribution, we see a good fit for 0.25 cm^{-1} , thus the scattering loss is found to be 1.1 dB/cm .

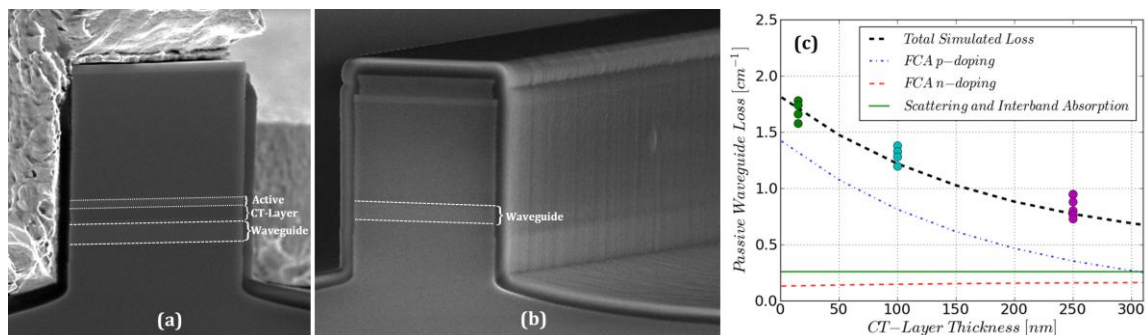


Fig. 2. Scanning electron microscopy (SEM) cross sectional image of (a) active and (b) passive waveguide sections of the 250 nm CT-layer design. (c) Passive waveguide loss simulated (lines) and measured (dots) for three different CT-layer thicknesses.

4. Characterization of Saturation Power and RF-linearity

The large signal gain, G_{LS} , and output saturation power, P_{so} , was determined by using two SOAs on the same waveguide. A continuous wave (CW) tunable laser at 1550 nm in-line with an EDFA and a variable attenuator was TE polarized and fiber coupled into the chip. First, the photocurrent in the front SOA is measured. Next, the front SOA is forward biased and the photocurrent in the back SOA is measured. Comparing the two photocurrents gives G_{LS} , while P_{so} is found by sweeping the input power and finding the 3dB G_{LS} roll off. Fig. 3(a) shows the measured results from a 1200 μm long SOA with $\Gamma=1.7\%$ (5 QWs, 1.36Q waveguide with 200 nm CT-layer thickness) at a terminal current density of 10 kA/cm². $P_{so}=19.1$ dBm and $G_{LS}=78$ dB/cm fits very well with the theoretical simulation in Fig. 1(b).

RF-photonics applications provided a large motivation for the high saturation and low loss integration platform developed in this work. Accordingly, the RF-linearity should also be characterized. The 3rd order non-linearity in SOAs is caused by four-wave mixing (FWM), with the most severe contribution from closely spaced tones (difference frequency, $w < \tau \sim 1\text{GHz}$) that mix through the carrier population oscillation (CPO) effect [2]. Fig.3(b) shows a schematic for the measurement setup used to measure the optical 3rd order output intercept point (OIP3). Two stable DFB lasers centered at 1550.02nm and spaced by 300 MHz, are input into the device with equal powers. The output is heterodyned with a tunable laser acting as a local oscillator (LO) tunable laser placed at 1550.00 nm, and the spectrum is measured on an electrical spectrum analyzer. The tone powers are normalized to the output of the SOA. The OIP3 point is extrapolated from the measured output fundamental tone power and the 3rd order intermodulation distortion (IMD3) tone powers by fitting lines with slopes of 1 and 3 as theory predicts [2]. For the same SOA design as above ($\Gamma=1.7\%$), we measured $P_{OIP3}=17$ dBm (the photodiode linearity was measured to be >30 dBm, and so did not affect the measurement). Although the NF have yet to be measured experimentally, we theoretically predict a NF of about 4 dB on-chip (i.e. no fiber coupling loss including). Using this NF and calculating the SFDR in the limit of a strong LO ($P_{LO} \gg P_{\text{signal}}$) and assuming a shot-noise limited system, an SOA SFDR of 112.6 dB-Hz^{2/3} is calculated. This is to our knowledge the highest SOA SFDR reported to date and is promising for active integration of RF-photonics devices [1,3].

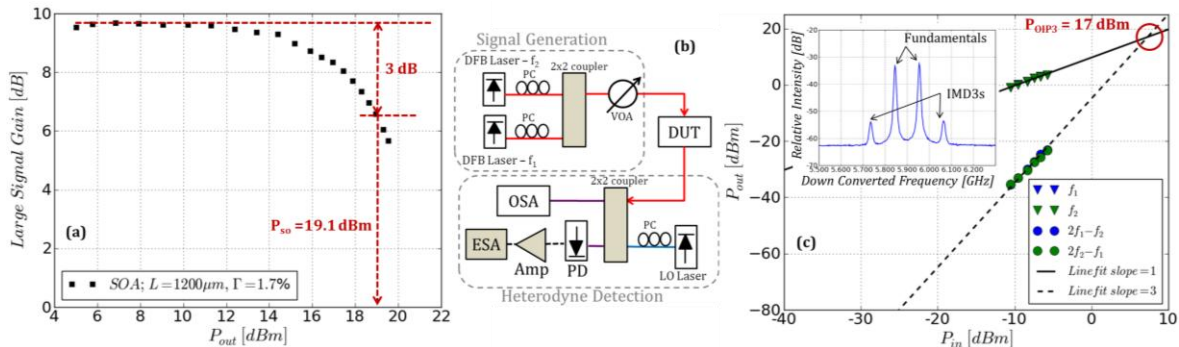


Fig.3. (a) Measurement of SOA DC characteristics, G_{LS} and P_{so} . (b) Schematic of measurement setup to characterize RF-linearity. (c) Optical fundamental and IMD3 tone powers extrapolated to find P_{OIP3} , inset show down-converted RF-spectrum.

5. Conclusion

We have presented an InGaAsP/InP integration platform capable of simultaneously achieving high P_s active regions and low loss passive regions. Using deeply etched waveguides, this platform is suitable for compact integration. We demonstrate deeply etched waveguides with passive loss as low as 3.5 dB/cm and P_s of 19.1 dBm while maintaining significant gain of 78 dB/cm. Finally we demonstrate state of the art RF-linearity results, with measured optical OIP3 power of 17 dBm suggesting SOA SFDR in the range of 112.6 dB-Hz^{2/3}.

6. References

- [1] R. S. Guzzon, E. J. Norberg and L. A. Coldren, "An SFDR Model for a Photonic Microwave Filter with Monolithically Integrated SOAs", submitted to European Conference on Optical Communication, (ECOC, 2011)
- [2] P. Berger, J. Bourderionnet, M. Alouini, F. Bretenaker, and D. Dolfi, "Theoretical study of spurious-free dynamic range on a tunable delay line based on slow light in SOA," *Opt. Exp.* **17**, 20584-20597 (2009).
- [3] E J. Norberg, R S. Guzzon, J S. Parker, L A. Johansson and L A. Coldren, "Programmable Photonic Microwave Filters Monolithically Integrated in InP/InGaAsP", *J. Lightwave Technol.*, in press, (2011).
- [4] P. W. Juodawlkis J. J. Plant, W. Loh, L. J. Missaggia, K. E. Jensen, and F. J. O'Donnell, "Packaged 1.5-um Quantum-Well SOA With 0.8-W Output Power and 5.5-dB Noise Figure," *Photon. Technol. Lett.* **21**, 1208-1211 (2009).
- [5] J. W. Raring, M. N. Sysak, A. T. Pedretti, M. Dummer, E. J. Skogen, J. S. Barton, S. P. Denbaars, and L. A. Coldren, "Advanced integration schemes for high-functionality/high-performance photonic integrated circuits," *Proceedings of SPIE*, (SPIE, 2006).
- [6] R. J. Deri, E. Kapon, "Low-loss III-V semiconductor optical waveguides," *J. Quantum Electronics* **27**, 626-640 (1991).